Abstract

1 Introduction

Seismic studies of the Canadian continental crust predominately analyze specific geological features or regions rather than taking a comprehensive and comparative inter-regional analysis. The primary reason for this is the poor resolution afforded by the seismic networks currently and historically deployed across Canada. The Canadian continental landmass is composed of at least fifteen large geological provinces as recognized by the Geological Survey of Canada (GSC). Each of these regions is itself complex and heterogeneous and often larger than most European nations. On top of this there is poor seismic coverage, roughly one seismic station per 25,000 km^2. Many of these stations are clustered near areas of geologic interest such as the Cascadia Subduction zone or population and research centres such as Southern Ontario or areas of significant resource interest like the diamondiferous Great Slave Lake area. This leaves vast areas of the Canadian landmass completely unsampled. Despite these limitations, a low resolution comprehensive and comparative study is still feasible for some of the geological regions comprising the Canadian continental crust. Direct comparison between the bulk average seismic properties of geological regions and between aggregated regions and global averages provide some new insight into the crustal composition of the Canadian landmass. The accumulated dataset also affords investigations into variations of bulk crustal parameters such as Poisson's Ratio and crustal thickness with age and tectonic environment as well as some basic statistical data on interesting crustal features.

This paper presents a comparative tour through the dataset accumulated from processing more than a decade worth of data from all available Canadian seismic stations. It begins with a discussion of the raw data itself followed by a review of the receiver function method and a more detailed explanation of the inversion algorithms used to produce the dataset. Three previous publications utilizing similar processing schemes provide unique subsets of data to compare with the values computed in this survey for quality assurance. ...

1.1 Geological and tectonic summary

1.2 Previous geophysical studies

2 Data and methods

Analysis of bulk Canadian continental crust requires estimates of crustal properties such as seismic-wave velocity and crustal thickness. This study draws on three sources for these crustal properties. The first and primary source for these estimates are data computed by processing raw seismograms into receiver functions and then inverting these RF's for parameter estimates. The other two datasets, the statistically compiled Crust 2.0 dataset and a compilation of pre-processed active source data, are used to qualify and compare with the primary dataset.

2.1 Teleseismic Data Set

The primary data utilized in this study are computed from teleseismic P-wave seismograms representing discrete seismic events. These events are comprised of seismic records representing more than 700 earthquake sources occuring between the years 2000 and 2012 at 343 broadband seismic stations across Canada. Seismic stations are selected from all available regional and national networks including CNSN, Polaris, FedNor and Chasme. Events are filtered by the epicentral distance from source to receiver with only the events within a 30 to 100 degree window being included. Seismic events are further filtered by hand picking those with reasonable signal to noise ratio and of sufficient impulsiveness that arrival times can be accurately measured. After selection and filtering more than 80,000 events are available for further processing.

The first stage of processing requires the transformation of teleseismic data into receiver functions. In its generic form this transformation involves deconvolving an approximation of the earthquake source from channels representing ground motion. The resulting waveform contains discrete pulses corrisponding to the arrivals of S-wave energy scattered from subsurface discontinuities. Resolving these peaks is essential to the success of the following inversion, therefore it is advantageous to rotate the seismogram components to seperate the P and S wave energy. This is accomplished by first rotating the N and E coordinates into radial and transverse dimensions and then

performing a wave field decomposition on the radial and vertical channels [Bostock, 1998]. The direct arrival of the signal on the resulting P wave componenent is used as an approximation to the source function as P waves are simpler and have a response closer to that of a delta function. This windowed source coda is deconvolved from the S wave component computed from the wave field decomposition.

An L_2 frequency domain deconvolution approach is used which has the advantages of computational efficiency as well as not requiring any assumptions about the noise in the data. This method performs a simultaneous deconvolution of N seismograms sharing a similar slowness to compute a single impulse response or receiver function $g(t)$.

$$g(t) = F^{-1}\left[G(\omega)\right] = F^{-}1\left[\frac{\sum_n^N S_n(\omega)P_n^*(\omega)}{\sum_n^N P_n(\omega)P_n^*(\omega)+\delta}\right], \tag{1}$$

where F^{-1} is the inverse Fourier transform, S_n represents the n^{th} S wave component, P_n is the windowed P wave component, * denotes the complex conjugatte and δ is the regularization parameter controlling the trade off between model smoothness and data misfit. The parameter δ is chosen programatically by minimizing the general cross validation function $GCV(\delta)$ which is given by

$$GCV(\delta) = \frac{\sum_n^N \sum_m^M \left(S_n(\omega_m) - P_n(\omega_m)G(\omega_m)\right)^2}{\left(NM - \sum_m^M X(\omega_m)\right)^2}, \tag{2}$$

where

$$X(\omega) = \frac{\sum_n^N P_n(\omega)P_n^*(\omega)}{\sum_n^N P_n(\omega)P_n^*(\omega)+\delta}, \tag{3}$$

and ω_m is the m^{th} frequency bin in the discrete Fourier transform.

All resulting receiver functions, $g(t)$, are filtered between 0.04Hz and 3.0Hz.

2.2 Vp/Vs method

A well tested and widely published method for extracting the ratio, $R = \frac{V_P}{V_S}$, where V_P is P-wave veolcity and V_S is S-wave velocity and crustal thickness, or depth to Moho, H, is outlined by Zhu and Kanamori [2000], hereafter ZK.

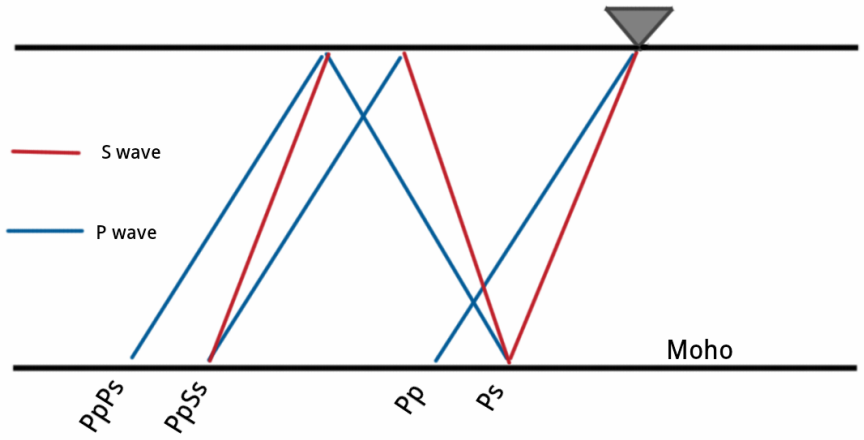

Figure 1: Schematic diagram illustrating geometry of phases for the velocity contrast representing the Moho

This method takes advantage of the differential arrival times between the S-wave reflected phases Ps, $PpPs$ $PsPs$, $PpSs$ and $PsSs$ and the direct P-wave arrival Pp, Figure 1. For a range of slowness values, p, the differential arrival times, $t(p)$, trace moveout curves for each phase arrival given by

$$t_{Ps}(p_i) = H\left[\sqrt{\left(\frac{V_p}{V_s}\right)^2 - p_i^2 V_p^2} - \sqrt{1 - p_i^2 V_P^2}\right] \tag{4}$$

$$t_{Pps}(p_i) = H\left[\sqrt{\left(\frac{V_p}{V_s}\right)^2 - p_i^2 V_p^2} + \sqrt{1 - p_i^2 V_P^2}\right] \tag{5}$$

$$t_{Pss}(p_i) = 2H\sqrt{\left(\frac{V_p}{V_s}\right)^2 - p_i^2 V_p^2} \tag{6}$$

where p_i is the slowness for the i^{th} receiver function. Since strong reflected phases occur at sharp velocity contrasts, the Moho, the boundary targeted by ZK, tends to be well representated on most RF's.

A well tested approach for calculating $R = \frac{V_P}{V_S}$ and H was employed by Zhu and Kanamori (2000). After deconvolution the signals are stacked and a gridsearch is performed using the travel time equations for different values of R and H and a spectrum of slowness. For each parameter combination the travel time functions output estimates for the differential arrival time of the S-component main and reflected phases. These times are used to pick the energy in each receiver function - with the large amplitudes at arrivals stacking to provide an estimate for the optimal parameter estimation.

2.3 Vp method

The stacking approach outlined above provides estimates for the parameters $R = \frac{V_P}{V_S}$ as well as crustal thickness H - which gives the depth of the Moho. A method which estimates V_P and V_S separately (Bostock, 2010) is also employed for select stations. This method makes use of the fact the dependence on H in the travel time equations can be removed if we divide the reflected phases by the main arrival.

$$t_{Pps}(p_i) = \frac{\sqrt{R^2 - p_i^2 V_P^2} + \sqrt{1 - p_i^2 V_P^2}}{\sqrt{R^2 - p_i^2 V_P^2} + \sqrt{1 - p_i^2 V_P^2}} t_{Ps}(p_i)$$

$$t_{Pss}(p_i) = \frac{2\sqrt{R^2 - p_i^2 V_P^2}}{\sqrt{R^2 - p_i^2 V_P^2} + \sqrt{1 - p_i^2 V_P^2}} t_{Ps}(p_i)$$

This has the advantage that no assumptions on V_P are necessary to perform the gridsearch and stack. A similar stacking method as the Zhu and Kanamori approach may be employed for t_{Pps} and t_{Pss} as long as an estimate for t_{Ps} exists. With estimates for R and V_P a simple line search along H can be made using all three undivided travel time equations.

(MOST LIKELY UNNECESSARY INFO) Several methods for choosing t_{Ps} are available. Direct arrival t_{Ps} should contain the largest fraction of energy out of the other phases and the moveout, depending on Moho depth, should be in the order of 3 to 6 seconds. Given this it is trivial to define a window and select the time corresponding to maximum amplitude. Another approach is to use max amplitude estimates as data in a non-linear optimization to find the R, V_P, and H which minimizes the residual between t_{Ps} and the data. The travel time equations are twice-differentiable so the quadratically convergent Newton's method may be employed. This approach

has the advantage that noise leading to poor maximum amplitude picks are effectively collapsed onto the curve corresponding to the travel time function. A third approach which offers picks along a travel time curve but better stability than the non-linear method is to perform a gridsearch with all three travel time functions, a full Kanamori stack. With the best estimates for R and H the t_{Ps} function can be found and used as input into the Bostock method. The trade-off is that the requirement for an initial V_P estimate for the initial stack introduces secondary V_P dependence into the system.

2.4 Vp database

Accompanying the processed estimates outlines above are data from controlled source experiments collected and compiled by external sources. The data was compiled by Mooney (personal communication, 2012).

3 Results

3.1 Comparisons

As regional studies exist which utilize similar methods and have corresponding parameter estimates for some of the stations used in this study it is possible to directly compare values to those previously published. A comprehensive study in the Hudson Bay region of the Canadian Shield (Thomson et. al., 2010) uses an approach similar to the Zhu and Kanamori method published estimates for H and $R = \frac{V_P}{V_S}$ for 35 stations. 5 stations with R estimates above 1.8 are removed due to the uncertainty surrounding these high values. There is strong correlation of 0.95 between crustal thickness values for both datasets (Figure 2). The velocity ratio data has a lower correlation of 0.5 (Figure 3). [Compare this value to uncertainty / deviation in the data?].

Directly comparing V_P estimates processed with the MB algorithm is not possible as this method has not been employed in publication. However, comparisons can be made to active source records for experiments within close proximity to a given seismic station (Figure 4. The correlation between these datasets is 0.235. [This is low, explain here?]. Another method of determining the reliability of estimates is to check the $\frac{V_P}{V_S}$ ratio taken from the Kanamori approach to the $\frac{V_P}{V_S}$ value computed from the MB approach. These

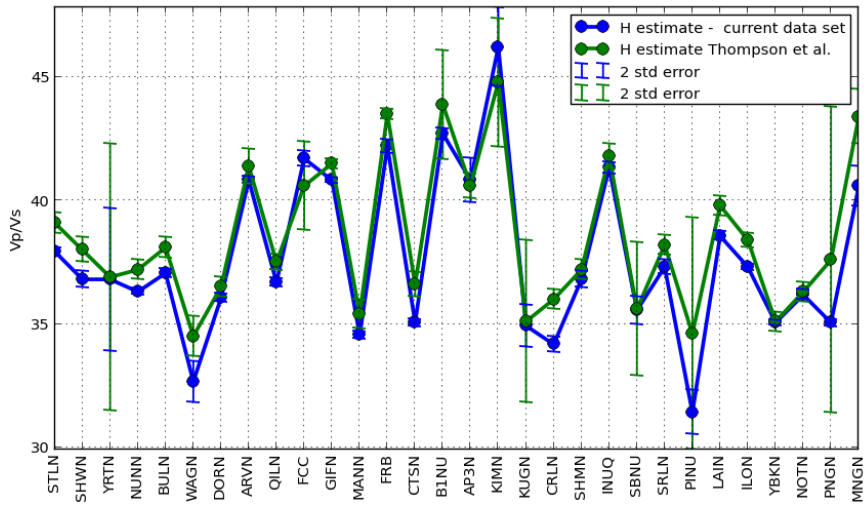

Figure 2: Comparison of crustal thickness H data from this study with data from Thomspson et. al. (2010). Data shows a Pearson correlation of 0.95

values, working with the same data, preprocessed using the same methods and tools should be equal. Selecting only those stations with an error of less than +/-0.05 R, 132 stations, we get a correlation of 0.57. Reducing the error tolerance and selecting stations with less than +/-0.01 R, leaving 31 of the cleanest stations, we get a correlation coefficient of 0.95.

3.2 Crustal Thickness

(MAY NOT INCLUDE)

- Jump in crustal thickness over the fault as you go from the Slave to the Rae or Churchill Province.
- Trend in Southern Ontario as we move north and up the St Lawrence Seaway.
- Appears to be secular variation in the North Eastern Churchill. As we move North and East we have thickening of continental crust.

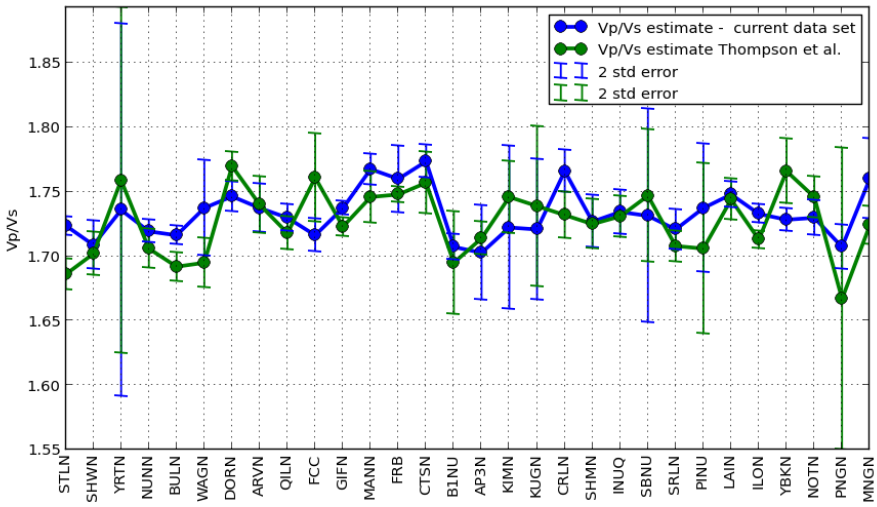

Figure 3: Comparison of V_P/V_R data from this study with data from Thompspson et. al. (2010). Data shows a Pearson correlation of 0.5

3.3 Vp/Vs

- reference Figure 5
- For perspective, the value for Quartzite is 1.65 and Basalt is 1.85.
- North East of the Slave province, has cluster of low Vp/Vs values in a semi circle of high values.
- Appears to be an shift throughout the Superior province from high Vp/Vs in the South to low Vp/Vs in the North East.
- Compare to Crust 2.0 overlay (Figure 6). Average value for Churchill province Vp/Vs is 1.73 while average value computed from Crust 2.0 is 1.77.

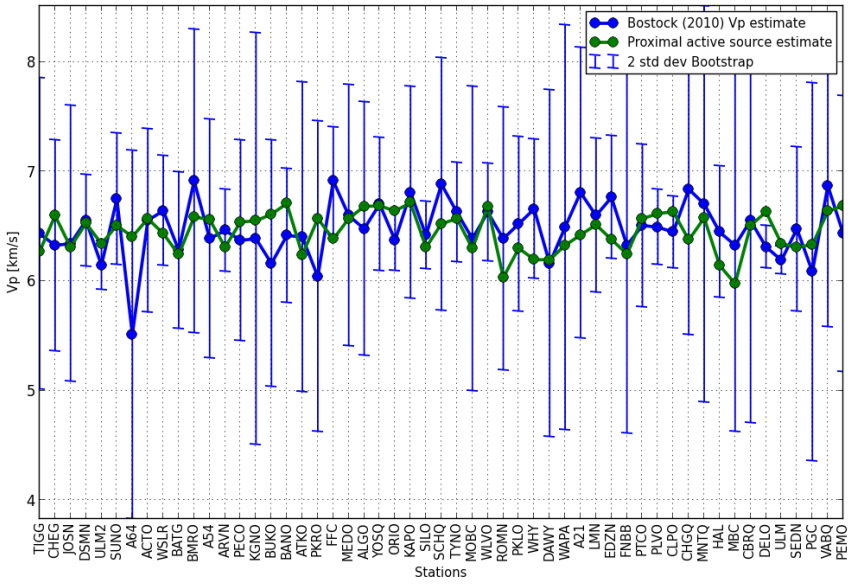

Figure 4: Comparison of V_P estimates from the MB algorithm with active source V_P recordings. Stations selected if active source experiment locations within 1 degree of latitude / longtitude.

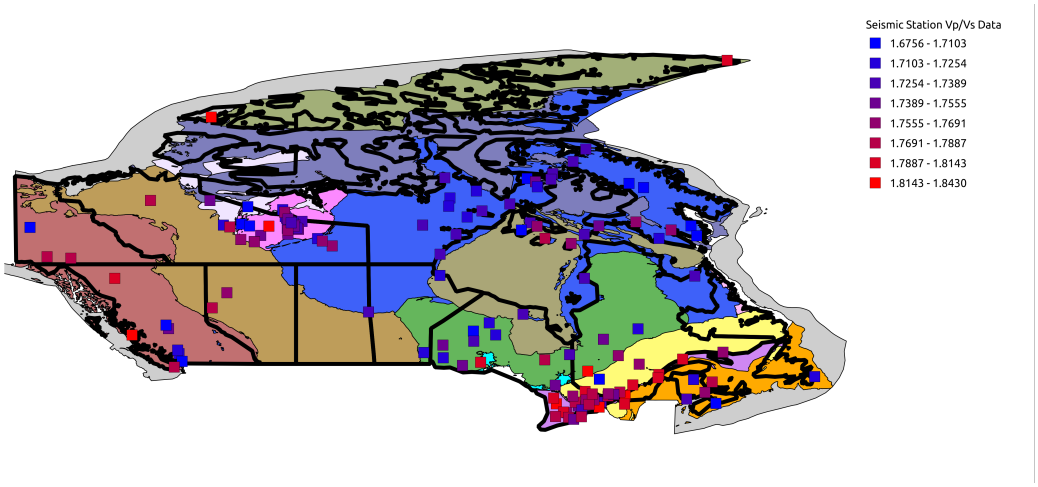

Figure 5:

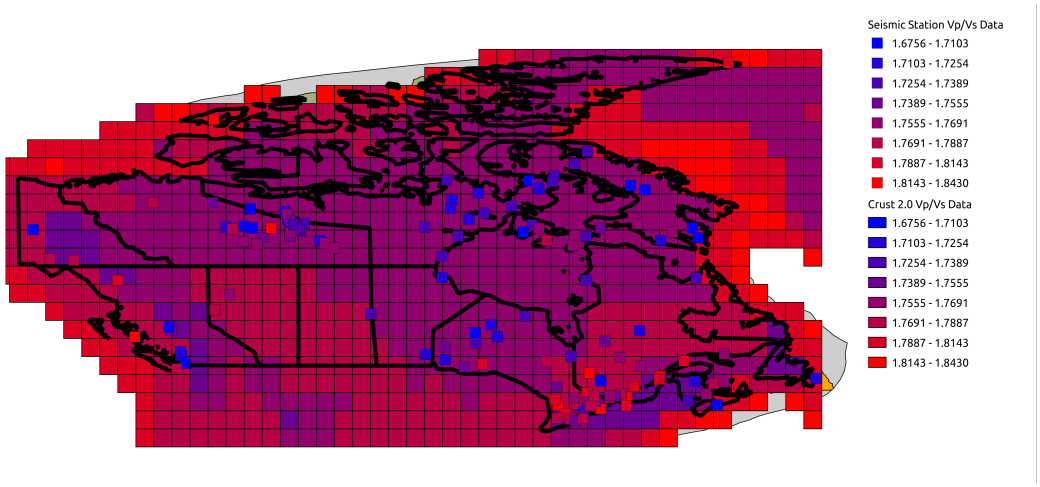

Figure 6:

4 Discussion

4.1 Canada

The preliminary interrogation of the data set yields the observation that the bulk Canadian Shield has lower Vp/Vs than anticipated. Previous experiments show crustal averages of 1.77 (Christensen and Mooney, 1995) and 1.78 (Zandt and Ammon, 1995). This compares to computed values of 1.73, 1.74, 1.795 for the Churchill, Superior and Grenville Provinces Vp/Vs ratios respectively.

(MIGHT NOT INCLUDE) The data bares out earlier results showing Proterozoic crust to have a higher seismic velocity ratio than Archean crust. This follows previous studies on crustal formation that have noted this trend in other regions (Durrheim and Mooney, 1991) . The increased crustal thickness of Proterozoic crust is clearly seen in the active source data while it not visible in data from processed seismic stations.

Further work on the Bostock-Kumar stacking approach is warranted from a look at the cleanest stations. Before it can be employed in large scale analysis additional denoising methods or alternative deconvolution techniques will need to be investigated to reduce the noise in the data.

4.2 Slave Province

¡Discussion on Slave Province¿

5 Conclusions

¡Conclusions here¿

References